Symmetry Breaking Charge Transfer as a Means to Study Electron Transfer With No Driving Force.

Michael Kellogg, Ali Akil, Daniel Sylvinson M. R., Laura Estergreen, Stephen E. Bradforth*, Mark E. Thompson*

Department of Chemistry, University of Southern California, Los Angeles, CA 90089, USA

Table of Contents

Supplementary Information 1 | Photoluminescence Measurements

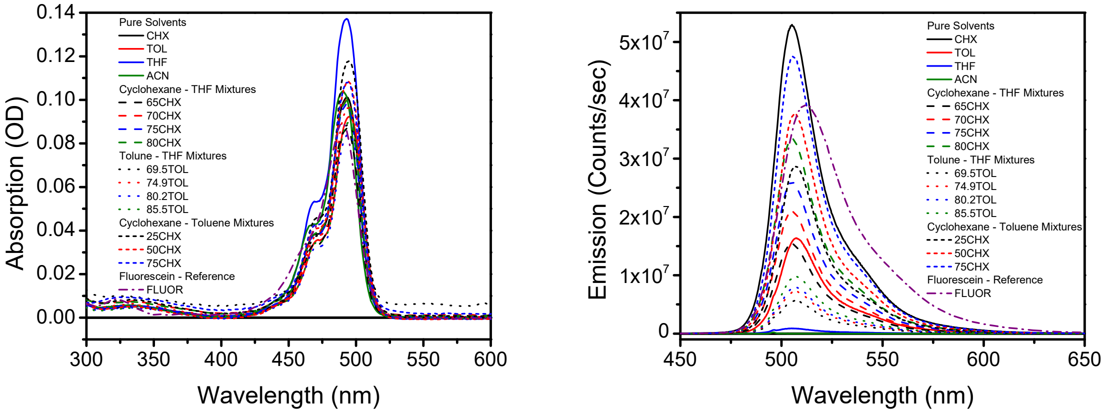

Figure S1 – Displayed are the steady state absorption (left) and emission (right) used in the PL measurements for **2**. In all solvents, **2** has a definitive max with a small red shoulder with some structure in the UV. The emission for **2** is mostly broad and featureless. The molecule exhibits very little solvatochromism save for solvation by acetonitrile in which the absorption maximum blue shifts to 490 nm from 494 nm. The absorption and emission spectra for fluorescein in 0.1M NaOH is also displayed.

Supplementary Information 2 | Transient Absorption

Section 1 | Pure Solvents

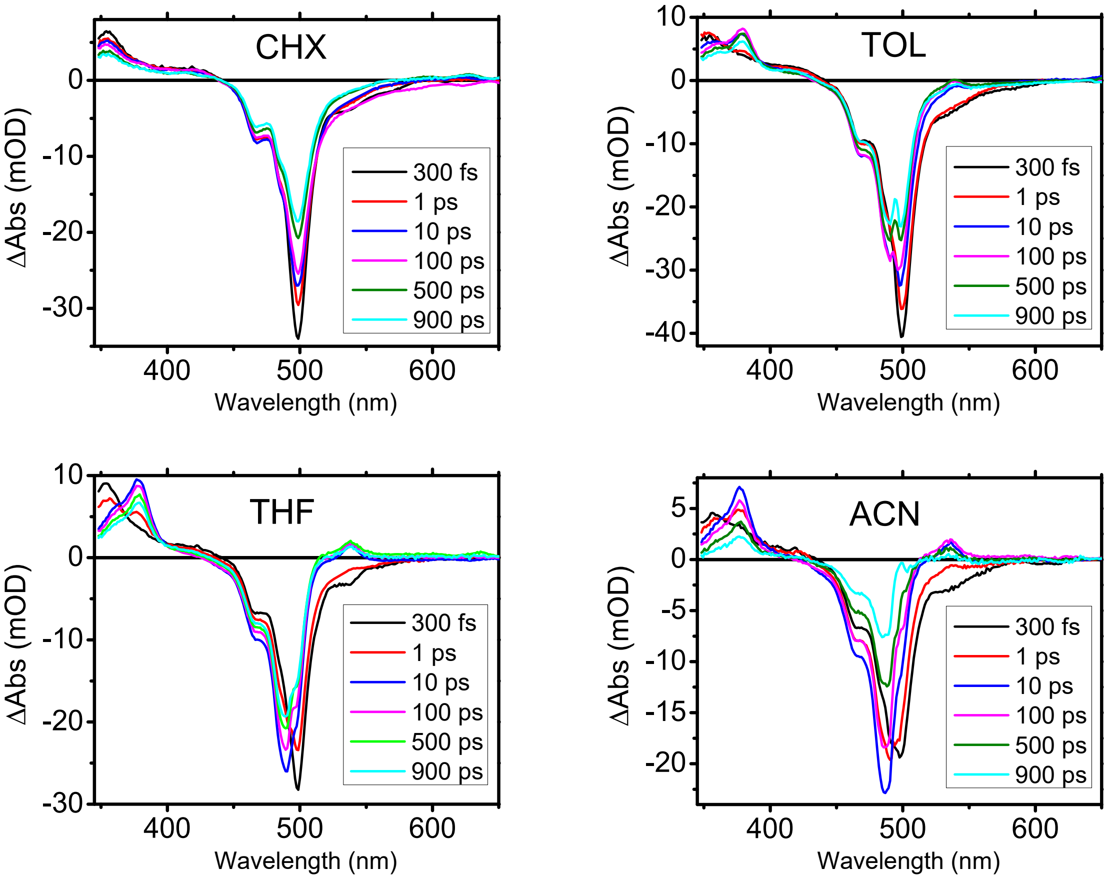

Figure S2 – Transient absorption spectra of **2** in varying pure solvents with respective solvent listed within each figure. The spectral features are as assigned as: LE excited state absorption (ESA) at 354nm, SBCT ESA at both 380 nm and 538 nm, ground state bleach (GSB) from 450 to 500 nm and stimulated emission (SE) from the LE state at 500 nm to 565 nm. As the excited state evolves, the bands at 380 and 538 nm grow in as the SE decreases. For CHX, there is no obvious spectral evolution forming within the excited state lifetime. There appears to be no evidence for SBCT formation. The ACN spectrum is seen to decay fastest of all solvents.

Interesting to note for each of the solvents where SBCT does occur, the GSB increases over time, indicating that another identical chromophore is being bleached due to its involvement in the SBCT process. This is most obvious in THF and ACN plots (10 ps traces) shown here.

Section 2 | Cyclohexane – THF Mixtures

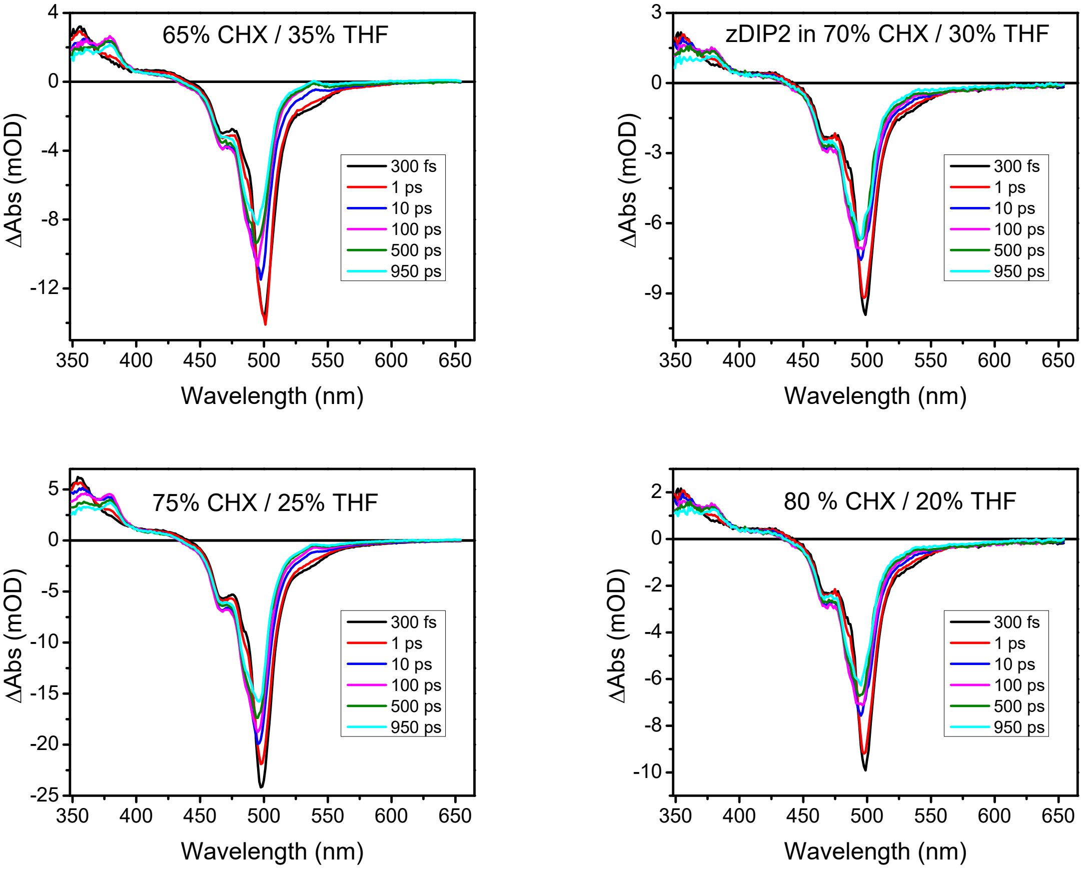

Figure S3 – Transient absorption spectra of **2** in varying ratios of CHX and THF. A slight increase in ESA of the SBCT state is seen as the solvent polarity increases (decreasing ratio of CHX compared to THF)

Section 3 | Toluene – THF Mixtures

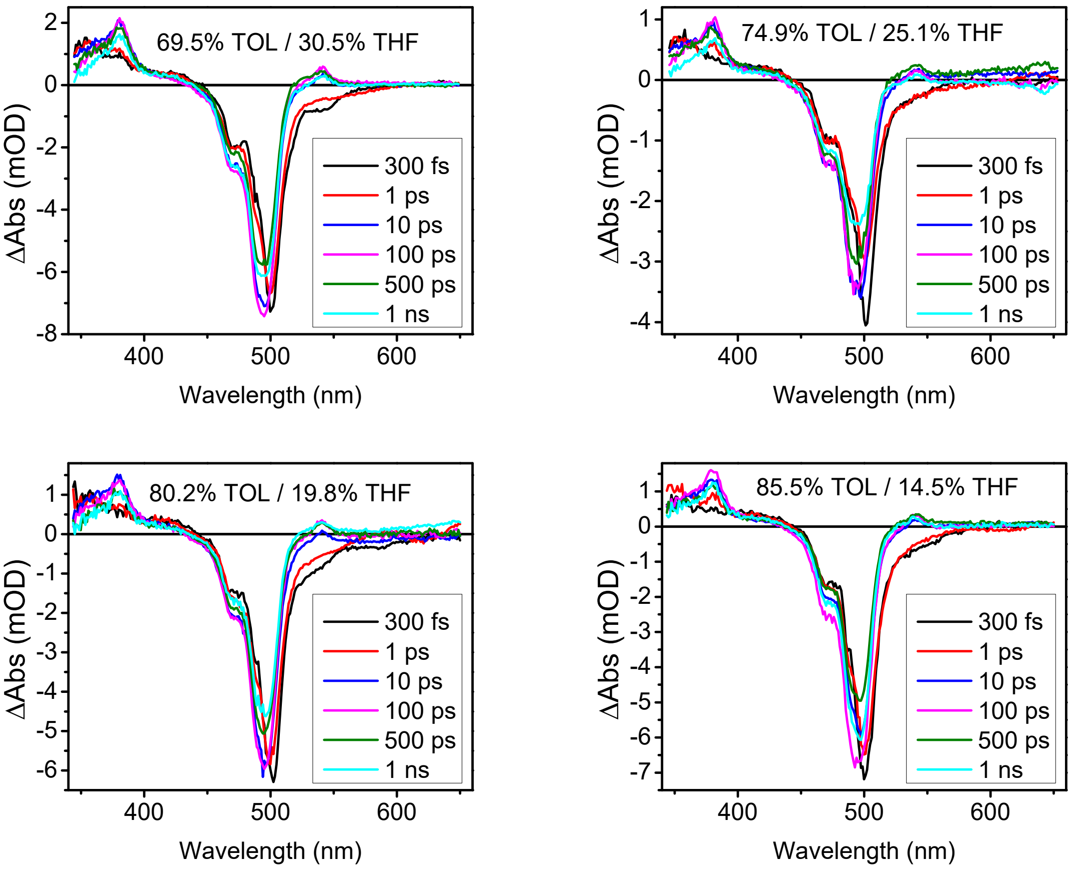

Figure S4 – Transient absorption spectra of **2** in varying ratios of TOL and THF. A slight increase in ESA of the SBCT state is seen as the solvent polarity increases (decreasing ratio of TOL compared to THF).

Section 4 | Toluene – Cyclohexane Mixtures

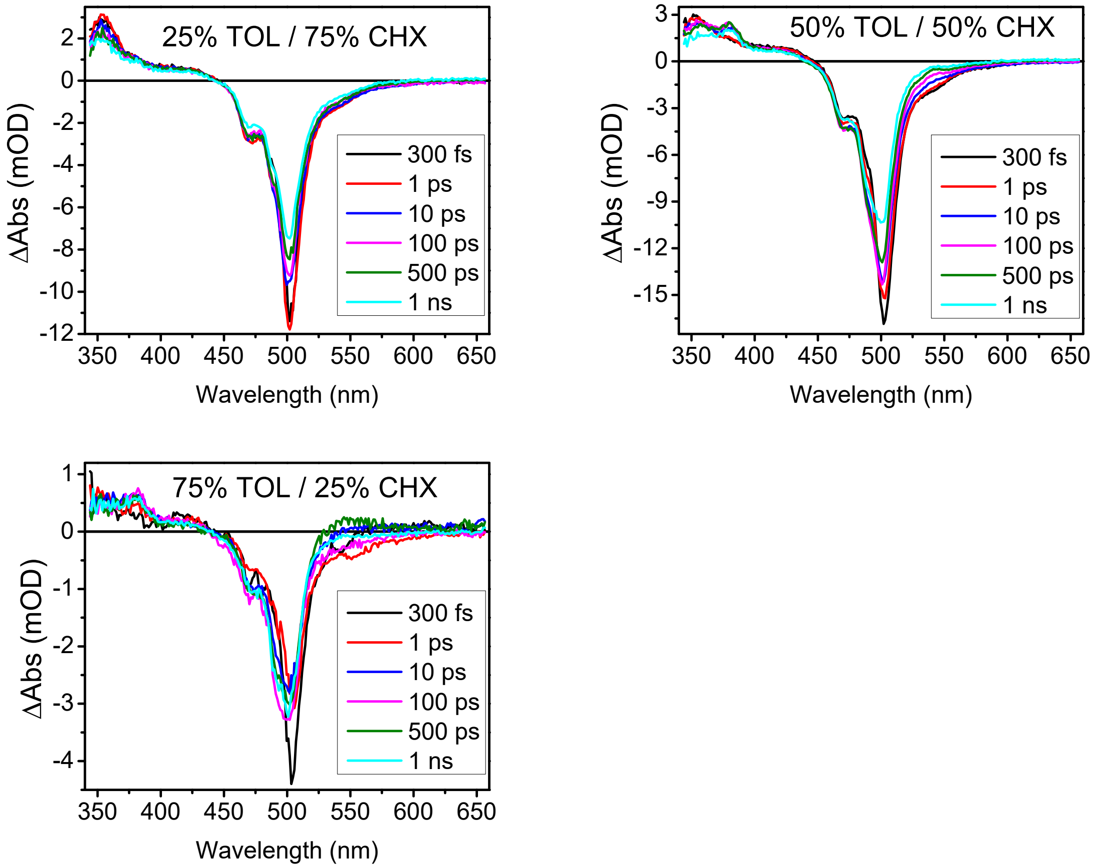

Figure S5 – Transient absorption spectra of **2** in varying ratios of TOL and CHX. In transitioning from 25% TOL to 50% TOL, the SBCT bands go from hardly noticeable to dominant (mostly at the 380 nm band).

Supplementary Information 3 | Time Correlated Single Photon Counting Measurements

In order to determine long time constants outside of the experimental window of the TA, TCSPC measurements were performed for each of the pure solvents. For the time constants, the long time constants are assigned τ_1 and short time constants are assigned τ_2. As such, the TCSPC will be more sensitive to the τ_1 values. Amplitudes of each exponential are assigned as A_x. Errors for each value as denoted by ε.

Section 1 | Cyclohexane

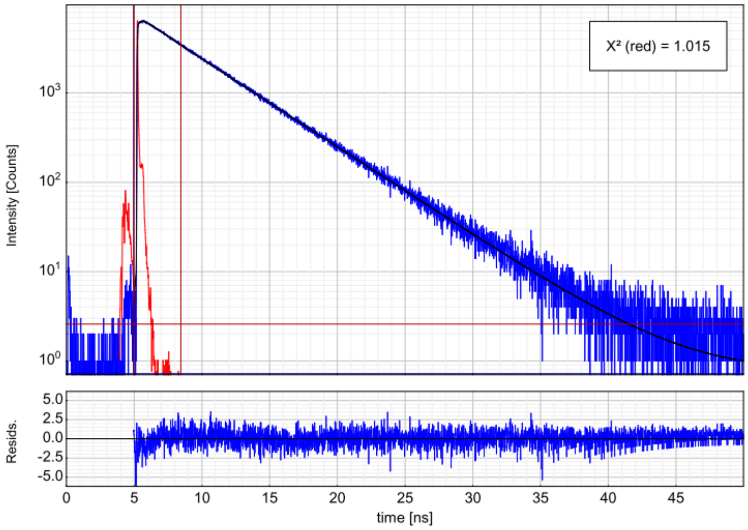

τ_1 (ns)	$\varepsilon(\tau_1)$ (ns)	A1 (Counts)	ε (A1) (Counts)
4.40	0.02	7740	50

Figure S6 – TCSPC measurement of **2** in CHX using 400 nm pump excitation, detecting at 550 nm with a power of 9 μW, a bandwidth of 4 nm and a collection time of 20 minutes. One exponential was fit considering the solvent is CHX and only the LE is populated. Therefore, only τ_1 is assigned. Each of the TCPSC measurements has an IRF of 22 ps.

Section 2 | Toluene

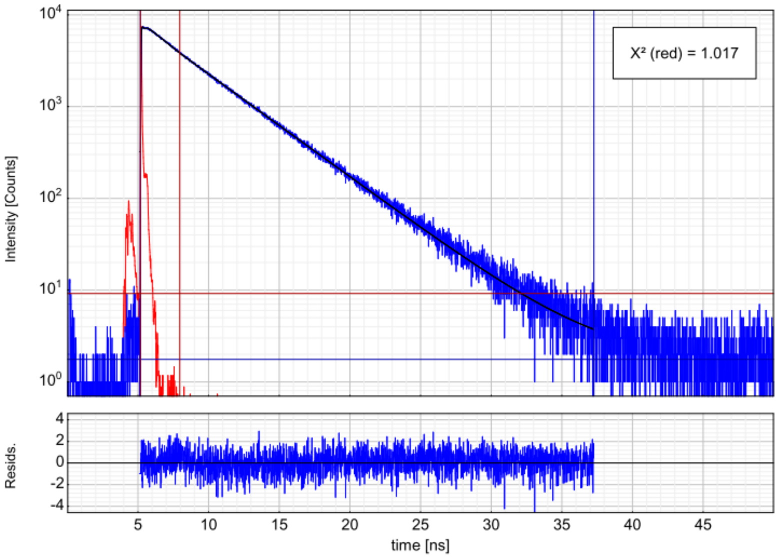

τ_1 (ns)	$\varepsilon(\tau_1)$ (ns)	τ_2 (ns)	$\varepsilon(\tau_2)$ (ns)	A1 (Counts)	ε (A1) (Counts)	A2 (Counts)	ε (A2) (Counts)
3.87	0.01	0.07	0.02	8740	50	2900	600

Figure S7 – TCSPC measurement of **2** in TOL using 400 nm pump excitation, detecting at 550 nm with a power of 4 μW, a bandwidth of 4nm and a collection time of 20 minutes. Two exponentials were fit to the data in contrast to CHX where there is no fast component due to SBCT.

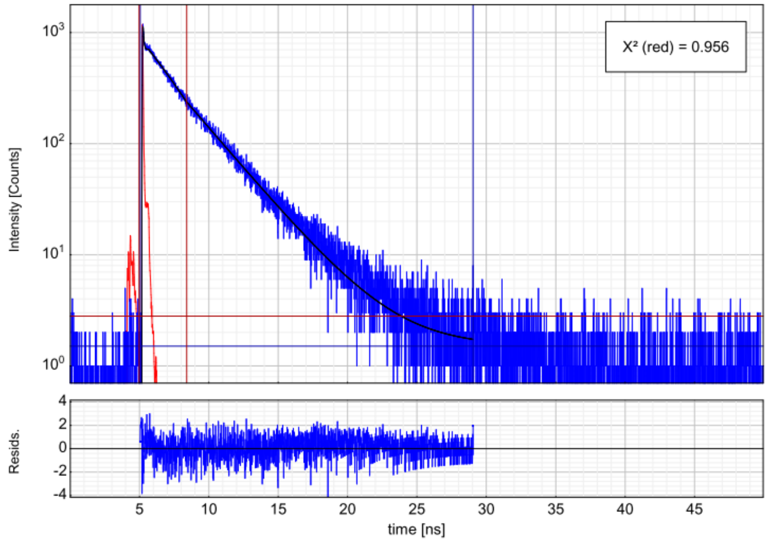

τ₁ (ns)	ε(τ₁) (ns)	τ₂ (ns)	ε(τ₂) (ns)	A1 (Counts)	ε(A1) (Counts)	A2 (Counts)	ε(A2) (Counts)
2.97	0.04	0.039	0.006	880	10	2400	300

Figure S8 – TCSPC measurement of **2** in THF using 400 nm pump excitation, detecting at 550 nm with a power of 93 μW, a bandwidth of 4 nm and a collection time of 20 minutes.

Section 4 | ACN

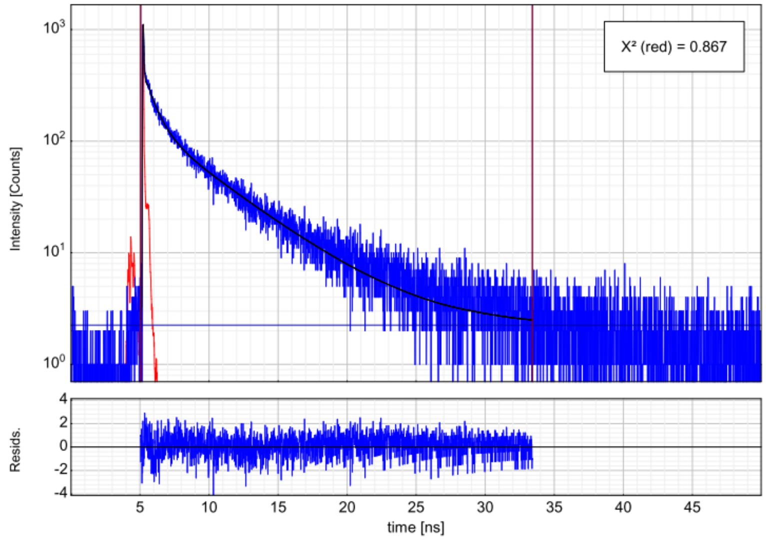

τ_1 (ns)	$\varepsilon(\tau_1)$ (ns)	τ_2 (ns)	$\varepsilon(\tau_2)$ (ns)	A1 (Counts)	ε(A1) (Counts)	A2 (Counts)	ε(A2) (Counts)
0.80	0.07	0.025	0.002	280	20	4800	500
		τ_3 (ns)	**$\varepsilon(\tau_3)$ (ns)**	**A3 (Counts)**	**ε(A3) (Counts)**		
		4.6	0.1	150	5		

Figure S9 – TCSPC measurement of **2** in ACN using 400 nm pump excitation, detecting at 550 nm with a power of 142 μW, a bandwidth of 4 nm and a collection time of 40 minutes. Three exponentials were required to fit the data. The extra exponential, assigned as an impurity, is listed as τ_3.

Section 5 | Fluorescein

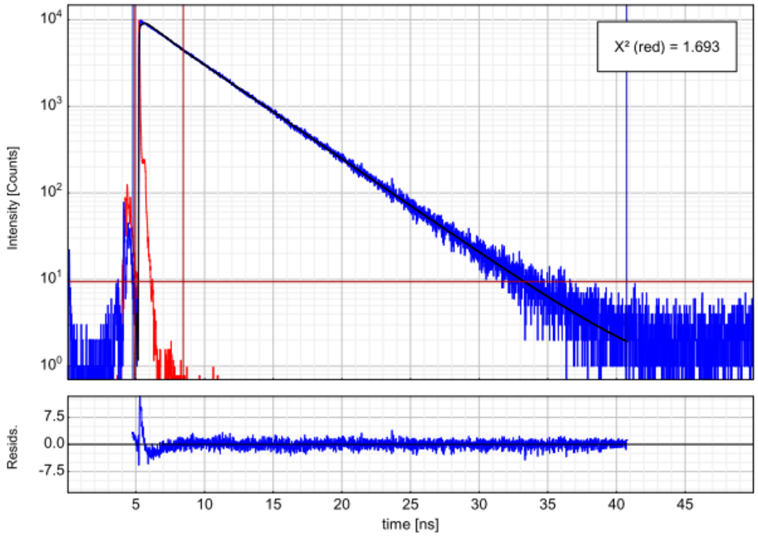

τ_1 (ns)	$\varepsilon(\tau_1)$ (ns)	A1 (Counts)	ε (A1) (Counts)
4.00	0.02	11150	70

Figure S10 – TCSPC measurement of fluorescein in 0.1M NaOH using 400 nm pump excitation, detecting at 550 nm with a power of 140 μW, a bandwidth of 4nm and a collection time of 20 minutes. One exponential was fit to the data. This experiment was performed in order to determine the amount of possible quenching by oxygen by comparing conditions under which the PL measurements were performed to the literature value. Our value of 4.00 ns compares well with reported value of 4.1 ± 0.1 ns.

Section 6 | TCSPC of **2** Decays Corrected

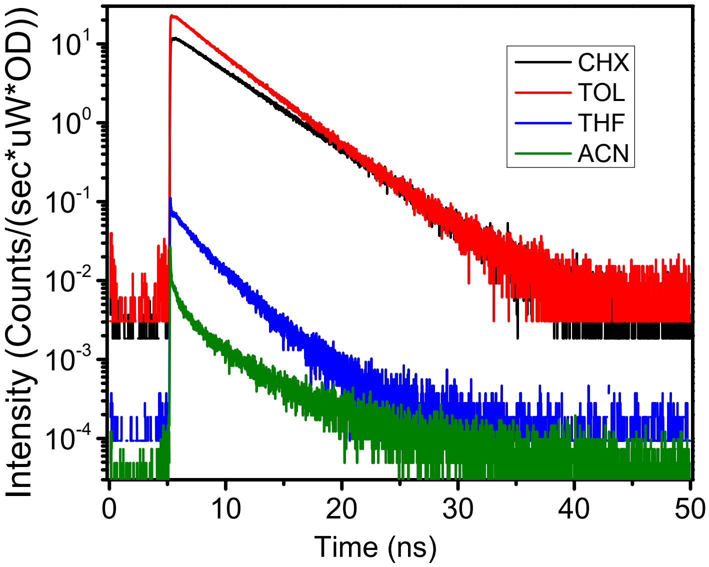

Figure S11 – TCSPC measurements of **2** in each of the four pure solvents where the differences in power, collection time and optical density (absorbance) were corrected to enable comparison of fluorescence intensity under like excitation conditions. There is substantial decay of fluorescence faster than the instrument response in the case of THF and ACN, consistent with the kinetic parameters revealed in the transient absorption analysis for these solvents.

Supplementary Information 4 | Summary of Rate Constants

Section 1 | Methodology for Rate Constant Fitting

Displayed below is the summary of the rate constants used to fit the TA, TCSPC and the PL measurements. The TA was performed in order to determine the fast rates, k_{ct} and k_{bet}, and determine ∆G. The TA measurements has sensitivity for processes that occur on the order of hundreds of femtoseconds to hundreds of picoseconds. However, processes like fluorescence and charge recombination to the ground state from the SBCT state occurs on the order of nanoseconds, times that are too long for TA to be able to pick up. However, TCSPC can be used, a technique that is sensitive in the nanosecond regime.

In CHX, SBCT is absent and only fluorescence (k_r) and internal conversion from the LE (k_{nr}) is present. From the QY (ϕ_{fl}) and TCSPC (τ) of **2** pure CHX, we pull both k_r and k_{nr}, according to equations S1 and S2.

$$\phi_{fl}^{CHX} = \frac{k_r}{k_r + k_{nr}} \qquad \text{Eqn S1}$$

$$\tau^{CHX} = \frac{1}{k_r + k_{nr}} \qquad \text{Eqn S2}$$

The values for k_r and k_{nr} are now fixed for all solvent systems. From the TCSPC, the value for k_{rec} can now be pulled from τ_2 according to equation S4, a simplification of equation S3 since k_{ct}, $k_{bet} >> k_r$, k_{nr}, k_{rec}.[28]

$$\frac{1}{\tau_{1,2}} = \frac{1}{2}(k_r + k_{nr} + k_{ct} + k_{bet} + k_{rec} \mp \sqrt{(k_{bet} + k_{rec} - k_r - k_{nr} - k_{ct})^2 + 4k_{ct}k_{bet}} \qquad \text{Eqn S3}$$

$$\frac{1}{\tau_1} = \frac{1}{2}(k_r + k_{nr} + k_{rec}) \qquad \text{Eqn S4}$$

Now, the TA data can be fit. The long time rate constants, (k_r + k_{nr}) and k_{rec} are fixed and the fast time constants are varied in the TA fitting program. Then k_{ct} and k_{bet} are determined. These results are listed in Table S1. The values for these are then plugged into Equation 1 and the PL quantum yield is back calculated from the kinetic parameters determined from the time-resolved data.

Section 2 | Summary of Rate Constants

Table S1 – Summary of Rate Constants for **2** in various solvents and solvent mixtures. All values are in inverse picoseconds (1/ps). Percent refers to the relative amount of the first listed solvent compared to the second one. The SBCT is not seen in pure CHX but is seen in mixtures with CHX. Therefore a k_{rec} for CHX mixtures exists. To determine the k_{rec} that CHX would have if SBCT was accessed, a straight line was taken between the k_{rec} values for TOL and THF and plotted as a function of $E_T(30)$. From this, a value for a pseudo-k_{rec} for CHX was imputed to be $1.2 \cdot 10^{-4}\, ps^{-1}$. From this value, k_{rec} for solvent mixtures containing CHX was calculated as a weighted average of the k_{rec} from CHX and the other solvent, either TOL or THF. These values are listed below.

Solvent	*Percent*	k_r	k_{nr}	k_{ct}	k_{bet}	k_{rec}
CHX	pure	$2.1 \cdot 10^{-4}$	$2.3 \cdot 10^{-5}$	0	0	$1.2 \cdot 10^{-4}$
TOL	pure	$2.1 \cdot 10^{-4}$	$2.3 \cdot 10^{-5}$	0.15	0.057	$2.9 \cdot 10^{-4}$
THF	pure	$2.1 \cdot 10^{-4}$	$2.3 \cdot 10^{-5}$	0.52	0.037	$4.5 \cdot 10^{-4}$
ACN	pure	$2.1 \cdot 10^{-4}$	$2.3 \cdot 10^{-5}$	0.93	0.047	$2.3 \cdot 10^{-3}$
CHX / THF	65	$2.1 \cdot 10^{-4}$	$2.3 \cdot 10^{-5}$	0.14	0.10	$2.4 \cdot 10^{-4}$
	70	$2.1 \cdot 10^{-4}$	$2.3 \cdot 10^{-5}$	0.17	0.11	$2.2 \cdot 10^{-4}$
	75	$2.1 \cdot 10^{-4}$	$2.3 \cdot 10^{-5}$	0.15	0.11	$2.0 \cdot 10^{-4}$
	80	$2.1 \cdot 10^{-4}$	$2.3 \cdot 10^{-5}$	0.11	0.11	$1.9 \cdot 10^{-4}$
TOL / THF	69.5	$2.1 \cdot 10^{-4}$	$2.3 \cdot 10^{-5}$	0.28	0.014	$3.4 \cdot 10^{-4}$
	74.9	$2.1 \cdot 10^{-4}$	$2.3 \cdot 10^{-5}$	0.28	0.022	$3.3 \cdot 10^{-4}$
	80.2	$2.1 \cdot 10^{-4}$	$2.3 \cdot 10^{-5}$	0.24	0.036	$3.2 \cdot 10^{-4}$
	85.5	$2.1 \cdot 10^{-4}$	$2.3 \cdot 10^{-5}$	0.24	0.029	$3.1 \cdot 10^{-4}$
CHX / TOL	25	$2.1 \cdot 10^{-4}$	$2.3 \cdot 10^{-5}$	0.20	0.22	$2.5 \cdot 10^{-4}$
	50	$2.1 \cdot 10^{-4}$	$2.3 \cdot 10^{-5}$	0.09	0.15	$2.1 \cdot 10^{-4}$
	75	$2.1 \cdot 10^{-4}$	$2.3 \cdot 10^{-5}$	0.05	0.20	$1.6 \cdot 10^{-4}$

Supplementary Information 5 | Derivation of Equations

Section 1 | Calculated QY from Rate Constants (Equation 1)

The model to describe this two-system used to fit the data comes from quencher kinetics. In our case, the quencher concentration is time dependent (SBCT). As such, the ϕ_{fl} used to describe the system is also derived from quencher kinetics.[1,28] Here, we will back calculate the provided equation to what matches in quencher kinetics. Equation 1 is displayed below.

$$\phi_{fl} = \frac{k_r(k_{bet}+k_{rec})}{(kr+knr)(k_{bet}+k_{rec})+4k_{ct}k_{rec}} \qquad \text{Eqn 1}$$

First we will invert equation 1 and separate to common denominator.

$$\frac{1}{\phi_{fl}} = \frac{(k_r+k_{nr})(k_{bet}+k_{rec})}{k_r(k_{bet}+k_{rec})} + \frac{k_{ct}k_{rec}}{k_r(k_{bet}+k_{rec})} \qquad \text{Eqn S5}$$

The like terms for the first fraction cancel.

$$\frac{1}{\phi_{fl}} = \frac{k_r+k_{nr}}{k_r} + \frac{k_{ct}k_{rec}}{k_r(k_{bet}+k_{rec})} \qquad \text{Eqn S6}$$

Where we see that the first term is actually just the reciprocal of the common quantum yield equation, the expected fluorescence from the LE state. The second term is ratio of the exciplex emission to the fluorescence emission.

$$\frac{1}{\phi_{fl}} = \frac{1}{\phi_0^F} + \frac{\phi^E}{\phi_0^F} \qquad \text{Eqn S7}$$

$$\phi_{fl}^E = \frac{k_{rec}}{k_{bet}+k_{rec}} \qquad \text{Eqn S8}$$

$$\phi_{fl}^F = \frac{k_{ct}}{k_r} \qquad \text{Eqn S9}$$

These equations relate back to what is found in quencher kinetics

Section 2 | Measured QY from Steady State Measurements (Equation 2)

In this paper, the QY of **2** in various solvents was measured via the relative QY method in which a reference, whose quantum yield is known, is used and compared against the sample of interest. To start, the total fluorescence intensity, E, is proportional to the intensity of amount of light absorbed and the fluorescence quantum yield (equation S10).

$$E = I_0(1 - 10^{-\epsilon bC})\phi_{fl} \qquad \text{Eqn S10}$$

where

$$f = 1 - 10^{-\epsilon bC} = 1 - 10^{-A} \qquad \text{Eqn S11}$$

so

$$E = I_0 f \phi_{fl} \qquad \text{Eqn S12}$$

Here, ϵ is the molar absorptivity, b is the optical pathlength, C is the concentration of fluorescing species, A is the species absorption, and ϕ_{fl} is the sample's fluorescence quantum yield. However, the sample will be contained in a cuvette in a solvent which has a differing refractive index, n_i compared to the refractive index which contains the detector, n_0. When fluorescent light passes from a higher refractive index to a lower refractive index (since $n_i > n_0$ most often), the light undergoes refraction as displayed in **Figure S12**. To correct this, consider a point source, S, from which light is emitting with an intensity of I (photons/sec). The intensity, I_i, emitted into the cone with the full angle, $2\theta_i$, is given by

$$I_i \cong \frac{4I}{\theta_i^2} \qquad \text{Eqn S13}$$

Where $sin\theta_i \cong \theta_i$ for small angle. There is no loss of photons going from first medium to second so the same amount of photons are present, they are just spread over a larger angle. Like Eqn S13, the intensity of light measured by the detector is given by

$$I_0 \cong \frac{4I}{\theta_0^2} \qquad \text{Eqn S14}$$

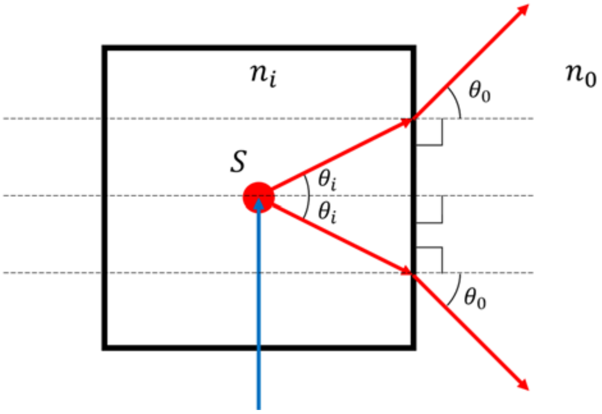

Figure S12. Refraction effect of light passing through cuvette after fluorescence. Blue arrow is excitation light, and red arrow is fluorescence. S is the point source.

Solving for I in eqn S14 and substituting it into eqn S13, we get

$$I_i = \frac{I_0 \theta_0^2}{\theta_i^2} \qquad \text{Eqn S15}$$

Then, we apply Snell's to find the effect of the refractive indices to get eqn 16

$$I_i = I_0 \left(\frac{\theta_0^2}{\theta_i^2}\right) = I_0 \left(\frac{n_i^2}{n_0^2}\right) \qquad \text{Eqn S16}$$

Now that the refractive indices have been corrected for, they can be plugged into Eqn S12.

$$E = I_0 f \phi_{fl} \left(\frac{n_0^2}{n_i^2}\right) \qquad \text{Eqn S17}$$

Solving for ϕ_{fl} we get equation S18

$$\phi_{fl} = \frac{E}{I_0 f} \cdot \left(\frac{n_i^2}{n_0^2}\right) \qquad \text{Eqn S18}$$

In order to get the final equation, equation 2, used in the paper, we must divide equation S18 by itself where one equation is for the sample and the other is the reference.

$$\frac{\phi_{fl}^S}{\phi_{fl}^R} = \frac{E_S f_R n_S^2}{E_R f_S n_R^2} \qquad \text{Eqn S19 (Equation 2)}$$

Which gets us back equation 2. The incoming light intensity, I_0, and refractive index outside the cuvette, n_0, will cancel. These light intensities only cancel if exciting at the same wavelength due to wavelength emission from the lamp. Since the fluorescence light is isotropic, the total emission light intensity and the amount measured by the detector are proportional to each other. This proportionality factor is the same for both reference and sample due to same distance from detector so this factor cancels.

Supplementary Information 6 | Geometry Optimizations

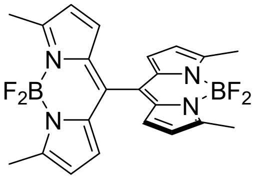

1

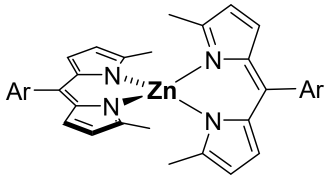

2

Table S2. Nuclear coordinates for calculated optimized ground state geometry of complex **1** (B3LYP / 6-31+G*)

ATOM	LABEL	X	Y	Z
1	C	1.42654644	-0.9317547	0.79893733
2	C	0.74610764	-0.0065601	0.00141955
3	C	1.44668355	0.90861224	-0.7934182
4	N	2.82426933	-0.970254	0.8346879
5	N	2.84330098	0.91974867	-0.8185582
6	B	3.76573331	-0.0307451	0.00818698
7	C	0.98020915	1.91636142	-1.6767279
8	C	3.24337838	1.88743156	-1.6743351
9	C	2.10134252	2.52326021	-2.2231352
10	C	0.93491567	-1.9305708	1.68165102
11	C	3.19808025	-1.9426776	1.69321938
12	C	-0.7493744	0.00646144	-0.0005594
13	C	-1.4457212	-0.9132565	-0.7916387
14	C	-1.4316462	0.9379576	0.78890109
15	N	-2.8291763	0.97508099	0.82012416
16	N	-2.843613	-0.926985	-0.8252375
17	B	-3.7675741	0.030528	-0.0019816
18	C	-3.2359473	-1.8992565	-1.6767747
19	C	-0.9728404	-1.9263431	-1.6669391
20	C	-2.0876792	-2.5377828	-2.2155546
21	C	-3.2065826	1.95375533	1.67100423
22	C	-0.9433042	1.94312272	1.66486447
23	C	-2.0486535	2.57327951	2.21142118
24	C	-4.6307879	2.29950213	1.96721518
25	H	-2.0555552	3.39051038	2.92118344
26	C	-4.6652847	-2.2212436	-1.9749901
27	H	-2.1071573	-3.3543851	-2.9258027
28	C	2.03761807	-2.5575237	2.23558805
29	C	4.62101637	-2.2873989	1.99590196
30	H	2.04201515	-3.3692966	2.95159598

31	H	2.12757739	3.33510059	-2.9383186
32	C	4.67991994	2.18946466	-1.9497338
33	F	4.56166817	-0.7947764	-0.8535659
34	F	4.56984321	0.71996298	0.873875
35	F	-4.5714448	-0.7169449	0.86644557
36	F	-4.5625772	0.78889379	-0.8688999
37	H	5.20207162	2.48180538	-1.0313601
38	H	4.76082133	3.00274673	-2.6761643
39	H	5.19816103	1.30828397	-2.3445657
40	H	5.32244662	-1.6633808	1.44264348
41	H	4.8160744	-3.3377556	1.74583719
42	H	4.81882842	-2.166864	3.06848738
43	H	-5.3548843	-1.5768214	-1.4303419
44	H	-4.8806745	-3.2641583	-1.7106626
45	H	-4.8611331	-2.1113	-3.0490478
46	H	-5.3302652	1.66732846	1.42082153
47	H	-4.8278266	3.34613121	1.70340679
48	H	-4.8302372	2.19197536	3.04085438
49	H	-0.0590527	2.14790605	-1.8684049
50	H	-0.1101454	-2.1412375	1.86596756
51	H	0.10100289	2.15671629	1.85010601
52	H	0.06799971	-2.1570399	-1.8511887

Table S3. Nuclear coordinates for calculated optimized SBCT state geometry of complex **1** (B3LYP / 6-31G)

ATOM	LABEL	X	Y	Z
1	C	1.43047559	-0.9362348	0.7987612
2	C	0.73429993	0.00198874	-0.0032734
3	C	1.42759643	0.94079312	-0.8059545
4	N	2.83184833	-0.9423942	0.81624496
5	N	2.82778683	0.94335997	-0.8177581
6	B	3.73213509	0.00667741	0.00071602
7	C	0.9844518	1.95584687	-1.6900029
8	C	3.2615506	1.93406336	-1.6840118
9	C	2.13723413	2.56671235	-2.2291251
10	C	0.98123832	-1.952104	1.67906634
11	C	3.2585695	-1.9364767	1.68252765
12	C	-0.7514841	0.00123941	-0.0016572
13	C	-1.4747417	-0.9182127	-0.7723122
14	C	-1.4732831	0.92131573	0.7695851
15	N	-2.8882698	0.9596451	0.79566798
16	N	-2.8898028	-0.9561854	-0.7960405
17	B	-3.8209059	0.00025404	0.00250373
18	C	-3.2762592	-1.9443474	-1.631574
19	C	-0.9913805	-1.9527768	-1.6505375
20	C	-2.0908045	-2.5841675	-2.1760529
21	C	-3.2730555	1.94925347	1.63025794
22	C	-0.9881461	1.95729777	1.64520668
23	C	-2.0865257	2.58979508	2.17154747
24	C	-4.6848334	2.29387102	1.92470587
25	H	-2.103478	3.41523213	2.865534
26	C	-4.6886316	-2.288573	-1.9237074
27	H	-2.1091405	-3.4082408	-2.8716261
28	C	2.12789216	-2.5670167	2.22102659
29	C	4.70551558	-2.224389	1.93928341
30	H	2.14808905	-3.3824251	2.9294206
31	H	2.16508038	3.37956866	-2.9399317
32	C	4.71308491	2.19724898	-1.9153767
33	F	4.59618344	-0.7507115	-0.876594
34	F	4.58248304	0.77433439	0.88187868
35	F	-4.6377716	-0.7457186	0.89919323
36	F	-4.6451894	0.74371532	-0.8895636
37	H	5.21602728	2.46146464	-0.9779006
38	H	4.84508005	3.01108493	-2.6339989
39	H	5.21648307	1.29974522	-2.2924561
40	H	5.35113006	-1.5667412	1.35815089

41	H	4.95268205	-3.26135	1.67788633
42	H	4.95098385	-2.0898268	3.00075659
43	H	-5.3909574	-1.6531239	-1.3878166
44	H	-4.878805	-3.3359091	-1.6561077
45	H	-4.8786791	-2.1996718	-3.0011304
46	H	-5.3881828	1.66082726	1.38731822
47	H	-4.8742032	3.3421949	1.66050417
48	H	-4.8740789	2.20185615	3.00203333
49	H	-0.0421434	2.20591877	-1.9125858
50	H	-0.047151	-2.200065	1.89602101
51	H	0.05608605	2.16007561	1.81478441
52	H	0.05250095	-2.1551553	-1.822709

Table S4. Nuclear coordinates for calculated optimized LE state geometry of complex **1** (B3LYP / 6-31G)

ATOM	LABEL	X	Y	Z
1	C	1.45193922	-1.0440738	0.6350224
2	C	0.74129836	-0.0033429	0.00053196
3	C	1.45577796	1.03503731	-0.6337348
4	N	2.86793003	-1.0686198	0.63894136
5	N	2.87175756	1.0554097	-0.6362324
6	B	3.78643521	-0.0071698	0.00318151
7	C	1.0089992	2.16844281	-1.3683061
8	C	3.29230588	2.15413588	-1.3311209
9	C	2.14869235	2.86037557	-1.7932861
10	C	1.00118008	-2.1769755	1.36811961
11	C	3.28455484	-2.1691531	1.33321941
12	C	-0.7396794	-0.0004494	0.00071966
13	C	-1.4546315	-1.0373456	-0.6351915
14	C	-1.4499458	1.0394366	0.63735723
15	N	-2.8659781	1.06465987	0.6414198
16	N	-2.8707595	-1.0571563	-0.6373721
17	B	-3.7849762	0.00460519	0.00410354
18	C	-3.2919573	-2.1545431	-1.3339142
19	C	-1.0085798	-2.1699095	-1.3715037
20	C	-2.1487052	-2.8606182	-1.7973769
21	C	-3.2820016	2.16395234	1.33809424
22	C	-0.9985547	2.17056123	1.37254174
23	C	-2.1354913	2.86600534	1.79945067
24	C	-4.7219697	2.48621203	1.53299803
25	H	-2.1605549	3.77389029	2.38287297
26	C	-4.7333616	-2.4714652	-1.5267839
27	H	-2.178063	-3.7679543	-2.3814457
28	C	2.13840262	-2.8725083	1.79362382
29	C	4.72468097	-2.4913054	1.52711623
30	H	2.16408194	-3.7814275	2.37540408
31	H	2.17751441	3.76867691	-2.3758792
32	C	4.7335309	2.47205616	-1.5236381
33	F	4.62998841	-0.6091963	-0.9937946
34	F	4.62677482	0.59370571	1.00365007
35	F	-4.6251224	-0.5979247	1.00375554
36	F	-4.6286363	0.60853449	-0.9915727
37	H	5.2336976	2.59992805	-0.5556103
38	H	4.85481189	3.3819379	-2.1153464
39	H	5.24645219	1.64142604	-2.0235108
40	H	5.24005442	-1.6609819	2.02499516

41	H	5.22486847	-2.6233076	0.55964427
42	H	4.84271632	-3.3999995	2.12126231
43	H	-5.2460055	-1.6395774	-2.0248812
44	H	-5.2333806	-2.6009465	-0.5588967
45	H	-4.8551734	-3.3800933	-2.1202801
46	H	-5.2374852	1.65506605	2.02933705
47	H	-5.2223272	2.62056586	0.56596643
48	H	-4.8395291	3.39369849	2.12914203
49	H	-0.0208243	2.4242116	-1.559483
50	H	-0.0295681	-2.4299566	1.55804439
51	H	0.03230363	2.42281879	1.56275228
52	H	0.02109675	-2.4257854	-1.5633285

Table S5. Nuclear coordinates for calculated optimized ground state geometry of complex **2** (B3LYP / 6-31+G*)

ATOM	LABEL	X	Y	Z
1	Zn	-2.575E-06	-0.0004668	0.00377648
2	N	1.3028148	1.10885686	-1.0255998
3	N	1.34647967	-1.0701339	1.02335325
4	N	-1.3410504	0.99445918	1.10097796
5	N	-1.3079935	-1.0478247	-1.0836197
6	C	2.6980149	0.96026148	-0.8719136
7	C	2.73519465	-0.8792381	0.85547854
8	C	3.31254549	0.04980559	-0.0114007
9	C	-2.7300262	0.79860565	0.94260952
10	C	-2.7024947	-0.9176434	-0.9073119
11	C	-3.3121746	-0.074836	0.02297494
12	C	-3.4113425	1.63779429	1.87963526
13	C	-1.1721542	1.91057614	2.08658075
14	C	-2.4408112	2.32850477	2.59211533
15	C	-3.3553721	-1.7896544	-1.8348131
16	C	-1.1086397	-1.9538954	-2.0725406
17	C	-2.3624559	-2.4344326	-2.5592626
18	C	1.09921469	2.08547532	-1.94372
19	C	3.34712563	1.89531751	-1.7388523
20	C	2.35122095	2.59572508	-2.4048669
21	C	1.18234214	-2.0524754	1.94420136
22	C	3.42113194	-1.7933022	1.71568334
23	C	2.45369473	-2.5236382	2.39223447
24	C	0.17903831	2.38843005	2.51344027
25	H	0.12101496	2.91660073	3.46963976
26	H	0.61044818	3.07801139	1.77531641
27	H	0.88157433	1.5544073	2.62131731
28	C	-0.268543	2.50107003	-2.3833694
29	H	-0.2333156	3.45885992	-2.9107386
30	H	-0.9492308	2.60054112	-1.5305611
31	H	-0.7120362	1.76098186	-3.0631901
32	C	0.25732101	-2.3297919	-2.5513177
33	H	0.22394149	-3.2516628	-3.1393713
34	H	0.94607489	-2.4789714	-1.7123373
35	H	0.6892566	-1.5442424	-3.1861028
36	C	-0.1679948	-2.5092576	2.39576956
37	H	-0.0967623	-3.4538416	2.94283449
38	H	-0.8451835	-2.6522997	1.54614125
39	H	-0.6376443	-1.7713112	3.05998636
40	H	-4.484413	1.70127663	1.99503197

41	H	-2.5915969	3.04890721	3.38274177
42	H	-4.3999305	-0.1003093	0.03057584
43	H	-4.4255026	-1.9089957	-1.9318154
44	H	-2.4889383	-3.1643799	-3.3453947
45	H	4.41695195	2.01701321	-1.8362487
46	H	2.47447443	3.38182775	-3.1354068
47	H	4.40048875	0.06631129	-0.0170328
48	H	4.49510077	-1.8819304	1.80266779
49	H	2.6084359	-3.3050237	3.12181325

Table S6. Nuclear coordinates for calculated optimized SBCT state geometry of complex **2** (B3LYP / 6-31G)

ATOM	LABEL	X	Y	Z
1	Zn	0.14606575	-0.0033689	0.00435442
2	N	1.29713912	1.13824817	-1.0458776
3	N	1.3746136	-1.0875201	1.03080899
4	N	-1.3465526	0.95540139	1.09380973
5	N	-1.3165243	-1.0363219	-1.0553559
6	C	2.69476587	0.99755785	-0.8962109
7	C	2.76113446	-0.876736	0.85449663
8	C	3.33334482	0.07597016	-0.02749
9	C	-2.7364033	0.83449602	0.89249909
10	C	-2.7110316	-0.8631888	-0.9414082
11	C	-3.337293	-0.001046	-0.0452926
12	C	-3.4277228	1.71496621	1.82849702
13	C	-1.1640333	1.84059082	2.0799144
14	C	-2.4631644	2.33899958	2.56362552
15	C	-3.3756073	-1.7377325	-1.9020364
16	C	-1.1069527	-1.9505036	-2.0087775
17	C	-2.3914697	-2.4109558	-2.5640864
18	C	1.07656612	2.14060115	-1.9844692
19	C	3.3209766	1.93041008	-1.7585862
20	C	2.30111126	2.63892108	-2.4336217
21	C	1.2230528	-2.0981312	1.97612536
22	C	3.44937315	-1.774209	1.70563664
23	C	2.4790961	-2.5321805	2.40163617
24	C	0.17927586	2.24674722	2.56396176
25	H	0.13257585	2.63223184	3.58561767
26	H	0.58415022	3.04008318	1.92094014
27	H	0.88164219	1.4111239	2.51644267
28	C	-0.3001687	2.5647466	-2.3985743
29	H	-0.2400726	3.35533011	-3.1542242
30	H	-0.8889441	2.96284643	-1.5592416
31	H	-0.8797384	1.73956837	-2.8370935
32	C	0.24856093	-2.386216	-2.4287076
33	H	0.22459709	-3.3888252	-2.8636259
34	H	0.94536686	-2.3651096	-1.5876471
35	H	0.64387166	-1.6986244	-3.1890199
36	C	-0.1235691	-2.5886361	2.41464313
37	H	-0.0115051	-3.379959	3.16334913
38	H	-0.7088612	-3.0070948	1.5831836
39	H	-0.7318366	-1.7933731	2.8690753
40	H	-4.499365	1.82442466	1.9004331

41	H	-2.5893294	3.06040171	3.35596403
42	H	-4.4227571	0.01814365	-0.0779866
43	H	-4.444327	-1.8146656	-2.0342888
44	H	-2.49541	-3.1468852	-3.3462531
45	H	4.38891419	2.06000224	-1.8657643
46	H	2.42990533	3.42498439	-3.165299
47	H	4.41883069	0.10363209	-0.0384454
48	H	4.52427253	-1.8497427	1.79308101
49	H	2.66172799	-3.3093414	3.13139727

Table S7. Nuclear coordinates for calculated optimized LE state geometry of complex **2** (B3LYP / 6-31G)

ATOM	LABEL	X	Y	Z
1	Zn	0.01048477	0.0029388	0.00238875
2	N	1.32012674	1.10547447	-1.0022182
3	N	1.36029874	-1.06794	0.99490258
4	N	-1.341781	0.9979456	1.0970975
5	N	-1.3083575	-1.0500231	-1.0771139
6	C	2.7406573	0.974686	-0.8629752
7	C	2.77603954	-0.8935664	0.84625257
8	C	3.38626346	0.04963766	-0.0108338
9	C	-2.7310176	0.80209337	0.93954539
10	C	-2.7029807	-0.9290521	-0.89518
11	C	-3.3134909	-0.0806446	0.02916773
12	C	-3.4130315	1.65438242	1.86423763
13	C	-1.173914	1.92813466	2.07042768
14	C	-2.4428254	2.35474212	2.56783476
15	C	-3.3542464	-1.8181683	-1.807569
16	C	-1.1074952	-1.9676881	-2.0557885
17	C	-2.3601555	-2.4647911	-2.5288534
18	C	1.09175603	2.09338085	-1.908351
19	C	3.36394388	1.92505787	-1.7213013
20	C	2.33964138	2.62377648	-2.3739484
21	C	1.16876179	-2.0617614	1.90342183
22	C	3.43351995	-1.8244106	1.70064456
23	C	2.43530424	-2.55296	2.3609925
24	C	0.17665274	2.41020458	2.49476637
25	H	0.11370369	2.96704868	3.43427195
26	H	0.6192593	3.07423916	1.73978379
27	H	0.87284639	1.57533711	2.63330922
28	C	-0.2827029	2.50875119	-2.3091254
29	H	-0.2487366	3.31462809	-3.0477364
30	H	-0.8665494	2.85973687	-1.4456915
31	H	-0.8470488	1.67016071	-2.7421151
32	C	0.25814712	-2.3386583	-2.5395299
33	H	0.2259389	-3.261134	-3.1267903
34	H	0.95093756	-2.483478	-1.7029978
35	H	0.68460127	-1.5514374	-3.1760486
36	C	-0.1902554	-2.5171278	2.31315766
37	H	-0.1281954	-3.3142047	3.05931603
38	H	-0.7649083	-2.8942937	1.45466013
39	H	-0.7787257	-1.6918637	2.73940685
40	H	-4.486246	1.72053343	1.97703261

41	H	-2.5938632	3.08624195	3.34818228
42	H	-4.401152	-0.1088171	0.03951776
43	H	-4.4239272	-1.947322	-1.8969161
44	H	-2.4850868	-3.2058666	-3.3047935
45	H	4.42960096	2.06328249	-1.8319954
46	H	2.44842454	3.41935441	-3.0977456
47	H	4.47142933	0.06666452	-0.0146351
48	H	4.503619	-1.9295341	1.80481483
49	H	2.57302643	-3.3436288	3.08522952

Supplementary Information 7 | Solvent Polarity Measurements

Table S8: Dielectric constants (ε) and $E_T(30)$ values for pure and mixed solvents. The dielectric constants are literature values.[1] The dielectric constants of mixed solvents are the weighted average of the dielectric constants of the two pure solvents. The $E_T(30)$ value for pure cyclohexane and acetonitrile were taken from the literature.[2] The $E_T(30)$ values for the cyclohexane (CHX) / tetrahydriofuran (THF) and toluene (TOL) / THF mixtures were determined experimentally using the absorption λ_{max} values for Reichardt's dye (2,6-Diphenyl-4-(2,4,6-triphenylpyridin-1-ium-1-yl)phenolate), as described in the literature.[2] The peak width of the dye in these solvent systems was quite broad, with a full width at half maximum of almost 250 nm. The breadth of the peak makes assigning λ_{max} problematic. In estimating the error bars for the CHX-THF and TOL-THF mixtures we used a λ_{max} value that is ± 4 nm. Due to the limited solubility of the dye in cyclohexane and TOL/CHX solvent mixtures that are rich in CHX, we could not reliably measure the $E_T(30)$ values for the mixtures. The TOL/CHX values in this table and used in our study are the weighted average for the $E_T(30)$ values for the two solvents. Using a weighted average for a solvent mixture has been established as a good estimate of the mixed solvent $E_T(30)$ when the two solvents have similar solvation properties of the dye,[3] which is expected in this case.

CHX – THF solvent mixture				
Ratio CHX/THF	λ_{max} /nm	$E_T(30)$ (kcal/mol)	+/- error in $E_T(30)$	ε
0/100	763	37.5	0.20	7.58
65/35	817	35.0	0.18	3.97
70/30	819	34.9	0.18	3.69
75/25	830	34.4	0.17	3.41
80/20	841	34.0	0.17	3.13
100/0	925	30.9[2]	0.16	2.02

TOL – THF solvent mixture

Ratio TOL/THF	λ_{max} /nm	$E_T(30)$ (kcal/mol)	+/- error in $E_T(30)$	ε
0/100	763	37.5	0.20	7.58
70/30	806	35.5	0.17	3.97
75/25	810	35.3	0.17	3.69
80/20	815	35.1	0.17	3.41
85/15	822	34.8	0.16	3.13
100/0	842	34.0	0.13	2.38

TOL – CHX solvent mixture

Ratio TOL/CHX	λ_{max} /nm	$E_T(30)$ (kcal/mol)	+/- error in $E_T(30)$*	ε
0/100	925[2]	30.9[2]	0.13	2.02
25/75	NA*	31.7	0.13	2.11
50/50	NA*	32.5	0.13	2.20
75/25	NA*	33.2	0.13	2.29
100/0	842	34.0	0.13	2.38

* Error bars for the $E_T(30)$ values were set at the values for the pre solvents.

1. Ware, W. R.; Watt, D.; Holmes, J. D. Exciple Photophysics. I. α-Cyanonaphthalene-Olefin System. *J. Am. Chem. Soc.* **1974**, *96* (26), 7853–7860.
2. A. A. Maryott and E. R. Smith, *Table of Dielectric Constants of Pure Liquids*, National Bureau of Standards, 1951.
3. C. Reichardt, *Chemical Reviews*, 1994, **94**.
4. P. M. E. Mancini, A. Terenzani, M. G. Gasparri and L. R. Vottero, *Journal of Physical Organic Chemistry*, 1995, **8**.